

PMCE: Probabilistic Multi-Granularity Semantics with Caption-Guided Enhancement for Few-Shot Learning

Jiaying Wu¹, Can Gao¹, Jinglu Hu², Hui Li¹, Xiaofeng Cao³ and Jingcai Guo^{4*}

¹Jiangsu Ocean University, China, ²Waseda University, Japan

³Tongji University, China, ⁴The Hong Kong Polytechnic University, Hong Kong SAR
{jiaying, 2024220911}@jou.edu.cn, jinglu@waseda.jp, lih@jou.edu.cn, xiaofengcao@tongji.edu.cn,
jc-jingcai.guo@polyu.edu.hk

Abstract

Few-shot learning aims to identify novel categories from only a handful of labeled samples, where prototypes estimated from scarce data are often biased and generalize poorly. Semantic-based methods alleviate this by introducing coarse class-level information, but they are mostly applied on the support side, leaving query representations unchanged. In this paper, we present PMCE, a Probabilistic few-shot framework that leverages Multi-granularity semantics with Caption-guided Enhancement. PMCE constructs a nonparametric knowledge bank that stores visual statistics for each category as well as CLIP-encoded class name embeddings of the base classes. At meta-test time, the most relevant base classes are retrieved based on the similarities of class name embeddings for each novel category. These statistics are then aggregated into category-specific prior information and fused with the support set prototypes via a simple MAP update. Simultaneously, a frozen BLIP captioner provides label-free instance-level image descriptions, and a lightweight enhancer trained on base classes optimizes both support prototypes and query features under an inductive protocol with a consistency regularization to stabilize noisy captions. Experiments on four benchmarks show that PMCE consistently improves over strong baselines, achieving up to **7.71%** absolute gain over the strongest semantic competitor on MiniImageNet in the 1-shot setting. Our code is available at <https://anonymous.4open.science/r/PMCE-275D>.

1 Introduction

Few-shot learning explores how to recognize novel categories from a small number of labeled samples. Despite the success of deep networks under large-scale supervision, performance often drops sharply in the few-shot regime, where decision boundaries can easily overfit a few supports and fail to transfer to novel classes. Traditional techniques such as

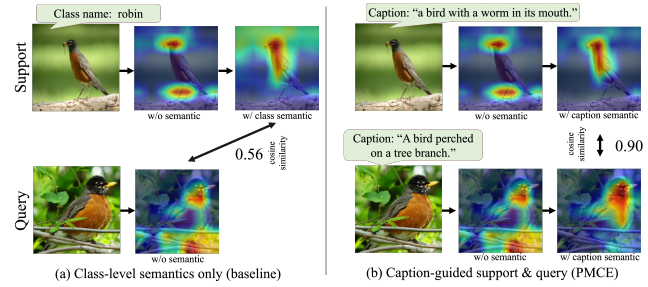


Figure 1: Comparison of semantic cues for support and query images. (a) **Class-level semantics only (baseline).** The support feature is modulated by its class name “robin”, while the query remains purely visual, leading to a relatively weak alignment between them (cosine similarity 0.56). (b) **Caption-guided support and query (PMCE).** BLIP-generated captions provide label-free instance-level semantics for both images, yielding more focused activation maps and a stronger support–query alignment (cosine similarity 0.90).

Matching Networks [Vinyals *et al.*, 2016], Prototypical Networks [Snell *et al.*, 2017], and MAML [Finn *et al.*, 2017], together with later strong baselines that revisit pre-training and episodic learning [Chen *et al.*, 2019; Tian *et al.*, 2020; Chen *et al.*, 2021a], have substantially improved the landscape. However, both benchmark studies and recent re-evaluations [Chen *et al.*, 2019; Luo *et al.*, 2023] suggest that the margins over simple baselines are still limited, especially for 1-shot tasks and visually diverse categories.

To compensate for the scarcity of labeled samples, semantic-based few-shot learning has become increasingly influential. These methods supplement visual features by introducing auxiliary information such as attributes, class names, human descriptions, and embeddings from visual language models into representations and classifiers [Xing *et al.*, 2019; Radford *et al.*, 2021; Chen *et al.*, 2023b; Zhang *et al.*, 2024a; Zhou *et al.*, 2025]. For example, attribute-based and cross-modal approaches adapt visual prototypes with class-level semantics [Xing *et al.*, 2019]. More recently, CLIP-driven prompt-based pipelines encode class names with templates and align them with image features [Radford *et al.*, 2021; Chen *et al.*, 2023b; Zhang *et al.*, 2024a; Chen *et al.*, 2026; Li and Wang, 2023; Dong *et al.*, 2025]. It is noteworthy that even lightweight methods using semantics can form

*Corresponding author

strong and robust baselines [Zhou *et al.*, 2025], which motivates us to consider how semantics should be leveraged to overcome the remaining bottlenecks.

This design choice matters most in the 1-shot scenarios, where prototypes are easily influenced by a single support example and query features often dominate the residual uncertainty. On one hand, distribution-based approaches, such as distribution calibration and MAP-style (Maximum A Posteriori) prototype correction [Yang *et al.*, 2021; Wang *et al.*, 2023a; Wu *et al.*, 2021; Wu and Hu, 2022], reuse base-class statistics to stabilize novel-class estimation. While effective, their priors are often chosen in the visual space via nearest neighbor search or manually written rules, rather than based on semantic associations between classes. On the other hand, most semantic-based approaches mainly rely on class-level text and inject it into support prototypes or classifier weights [Xing *et al.*, 2019; Chen *et al.*, 2023b; Zhang *et al.*, 2024a], whereas query features are rarely updated when the model cannot rely on query-set statistics. Therefore, even with strong semantic baselines, performance can be limited by the mismatch between noisy supporting prototypes and purely visual queries.

In this work, we present PMCE, a few-shot framework that uses multi-granularity semantics to address the problems of biased prototypes and weak query representations in 1-shot recognition. PMCE assigns different roles to different semantics. Class-name embeddings are used to identify semantically relevant base categories and turn their statistics into class-specific priors for prototype calibration, while label-free captions provide instance-level cues that refine both support-side prototypes and query features in the same representation space. We train only a lightweight enhancement module on base classes and keep the backbone and vision-language encoders frozen, so improvements mainly come from how semantics are injected rather than from increasing model capacity. Extensive experiments on four benchmarks with two backbones validate the effectiveness of this design, especially in the 1-shot setting. Our contributions are summarized as follows:

- We propose a PMCE method that combines semantic-based prior calibration with description-based image representation refinement without requiring adaptation using query set statistics.
- We leverage class-name semantics to obtain class-specific prior information and enhance the support set and query representation with unlabeled descriptions, thereby constructing a more consistent space for prototype-based inference.
- We introduce a lightweight consistency regularizer and achieve consistent improvements across four benchmarks using two backbone networks, with the most significant improvement on the 1-shot tasks.

2 Related Work

In this section, we present three main streams for existing representative few-shot learning approaches and followed by several methods based on Vision-language models.

Metric- and distribution-based few-shot learning. Few-shot learning has been extensively explored with techniques like transferable metric spaces and meta-learned initialization. These methods include Matching Networks [Vinyals *et al.*, 2016], Prototypical Networks [Snell *et al.*, 2017], MAML [Finn *et al.*, 2017], and later strong baselines that revisit pre-training and episodic learning [Chen *et al.*, 2019; Tian *et al.*, 2020; Chen *et al.*, 2021a]. Recent work further improves representations and distance functions, such as method FGFL with frequency guidance [Cheng *et al.*, 2023] and CPEA with class-aware patch embeddings [Hao *et al.*, 2023]. Another line models feature distributions and transfers base-class statistics to novel classes, including distribution calibration [Yang *et al.*, 2022b] and MAP-style prototype estimation [Wu *et al.*, 2021; Wu and Hu, 2022]. While effective, they often rely on visual similarities and heuristic selections in the feature space. PMCE follows this calibration perspective, but selects prior candidates with CLIP-encoded class-name semantics and incorporates it with caption-guided feature refinement.

Semantic-based few-shot learning. Semantic-based methods incorporate semantics like attributes, word vectors, or text embeddings to compensate for limited visual examples [Chen *et al.*, 2021b; Chen *et al.*, 2025c; Chen *et al.*, 2023d; Chen *et al.*, 2023c; Guo and Guo, 2020; Guo *et al.*, 2023; Guo *et al.*, 2024c; Guo *et al.*, 2021; Lu *et al.*, 2023; Guo *et al.*, 2024b; Guo *et al.*, 2024al]. For example, AM3 [Xing *et al.*, 2019] adapts visual prototypes with class-level semantics. Based on CLIP [Radford *et al.*, 2021], BMI [Li and Wang, 2023], SP-CLIP [Chen *et al.*, 2023b], SemFew [Zhang *et al.*, 2024a] and PRSN [Dong *et al.*, 2025] encode class names with prompts and inject text features into metric pipelines or prototype optimization. Most approaches remain class-centric and mainly intervene on support prototypes or classifier weights, while the query representation is often left unchanged or only processed through transduction clues. In PMCE, class-name semantics guide prior selection, and captions provide instance-level cues to optimize both support and query streams in the same metric space.

Vision-language models. Vision-language pre-training provides rich textual signals for visual recognition. CLIP aligns images and text from large-scale image-caption pairs [Radford *et al.*, 2021], and BLIP further improves description generation and integrates visual language representations. [Li *et al.*, 2022]. Recently, several few-shot work use CLIP textual features to represent category names or manually designed prompts [Chen *et al.*, 2023b; Zhang *et al.*, 2024a], while automatic description generation has not been extensively explored under standard inductive evaluation. PMCE leverages BLIP-generated captions as label-free instance semantics and combines them with class-level CLIP semantics, enabling semantics-guided MAP calibration and caption-guided enhancement without using the joint distribution of unlabeled queries.

3 Preliminaries

In this section, we explain the few-shot setting and review the MAP-based prototype calibration that our method builds on.

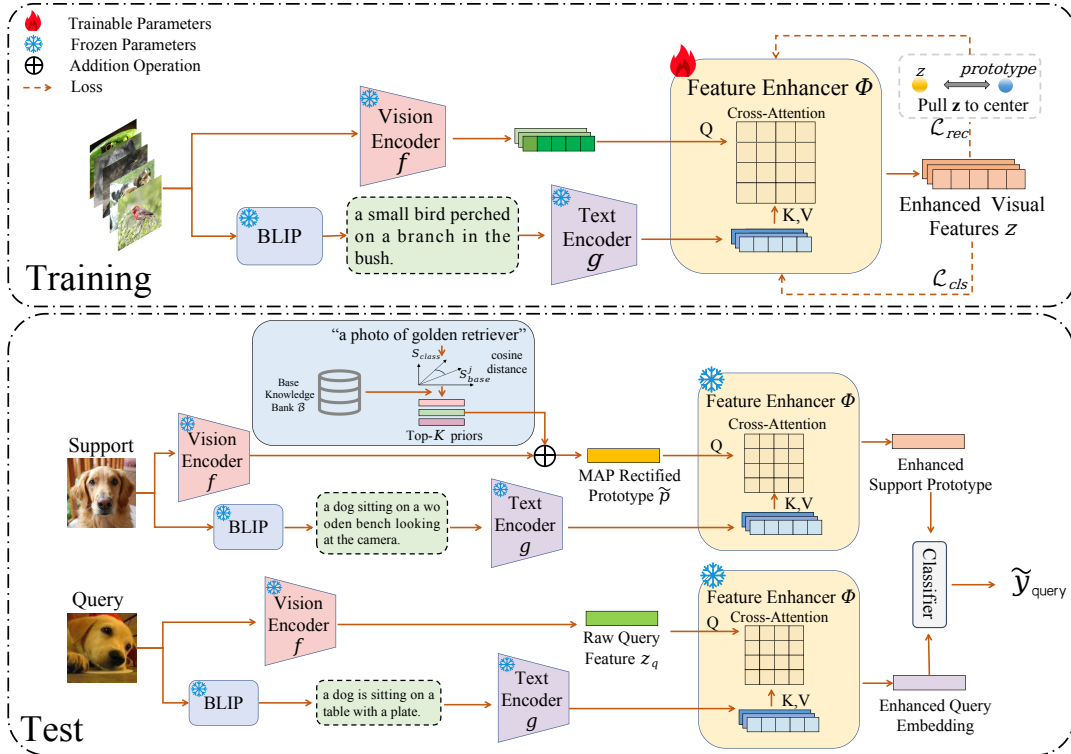


Figure 2: Overall framework of PMCE. **Training stage:** On base classes, we build a non-parametric knowledge bank that stores class-wise visual statistics and class-name embeddings, and train a caption-guided enhancer Φ by fusing visual features from f with BLIP-generated caption semantics from g . **Test stage:** (1) extract visual features and label-free captions for both supports and queries; (2) use class-name semantics to retrieve related base classes from the knowledge bank and obtain a class-specific prior, which is fused with the support prototype in a MAP-style update to get \tilde{p} ; (3) apply Φ to enhance \tilde{p} with aggregated support captions and to enhance query features with their own captions, and perform metric-based classification in the aligned feature space.

3.1 Problem Setting

In the standard few-shot setting, we have a base set $\mathcal{D}_b = \{(x_i, y_i)\}_{i=1}^{|\mathcal{D}_b|} \subset \mathcal{X} \times \mathcal{C}_b$ and a novel set $\mathcal{D}_n = \{(x_i, y_i)\}_{i=1}^{|\mathcal{D}_n|} \subset \mathcal{X} \times \mathcal{C}_n$, where $\mathcal{C}_b \cap \mathcal{C}_n = \emptyset$. \mathcal{D}_b provides abundant annotated data needed to train the visual backbone and the enhancement module, while \mathcal{D}_n is used only at meta-test time.

At meta-test time, we evaluate the performance on the N -way K -shot tasks. Each task contains a support set $\mathcal{S} = \{(x_i, y_i)\}_{i=1}^{N \times K}$ and a query set $\mathcal{Q} = \{(x_j, y_j)\}_{j=1}^{N \times M}$, where M is the number of query samples per class. Given support set \mathcal{S} and a query image x_q , the goal is to predict its label by

$$\hat{y}_q = \arg \max_{c \in \mathcal{C}} p(c | x_q, \mathcal{S}, \mathcal{D}_b), \quad (1)$$

where \mathcal{C} denotes the set of N classes sampled in the current episode.

3.2 MAP-based Prototype Calibration

Following [Wu *et al.*, 2021; Wu and Hu, 2022], we construct a visual knowledge bank based on the priors from base set. Specifically, for each base class $j \in \mathcal{C}_b$, we store its mean feature

$$\mu_j = \frac{1}{|\mathcal{D}_b^j|} \sum_{(x_i, y_i) \in \mathcal{D}_b^j} f_\theta(x_i), \quad (2)$$

where $\mathcal{D}_b^j = \{(x_i, y_i) \in \mathcal{D}_b \mid y_i = j\}$.

For a novel class c in an episode, p_{init}^c is the empirical prototype calculated from the mean of its support features. Given a class-specific prior mean μ_{prior}^c obtained from the knowledge bank, we calibrate the prototype by a MAP estimator under the Gaussian assumptions, which admits a closed-form convex combination:

$$\tilde{p}^c = \alpha p_{\text{init}}^c + (1 - \alpha) \mu_{\text{prior}}^c, \quad (3)$$

where $\alpha \in [0, 1]$ controls the strength of the prior.

4 Method

In this section, we present the semantics-guides prior selection strategy, the caption-guided enhancer, and the training objective in PMCE, the overall framework is shown in Fig. 2.

4.1 Semantics-Guided Prior Selection

We demonstrate the prior selection with CLIP class-name semantics for MAP prototype calibration in Eq. (3).

Class-level semantics on base classes. Let n_y be the natural language name of class y . We follow the CLIP-style prompting strategy and encode

$$s_{\text{class}}^y = g_\phi(\text{"a photo of a } n_y\text{"}) \in \mathbb{R}^{d_t}, \quad (4)$$

which provides a coarse description of category y . For each base class j , we store its mean feature μ_j and class-name embedding $s_{\text{base}}^j = s_{\text{class}}^j$ in a non-parametric semantic knowledge bank

$$\mathcal{B} = \{(\mu_j, s_{\text{base}}^j)\}_{j=1}^{|\mathcal{C}_b|}. \quad (5)$$

Prior selection for novel classes. At meta-test time, for a novel class c with class name n_c and embedding s_{class}^c , we measure its similarity to each base class via cosine similarity:

$$\text{score}_j = \frac{s_{\text{class}}^c \cdot s_{\text{base}}^j}{\|s_{\text{class}}^c\| \|s_{\text{base}}^j\|}. \quad (6)$$

We then select the indices of the top- K base classes to obtain a neighbor set \mathcal{N}_{top} and aggregate their visual means into a class-specific prior. Instead of uniform averaging, we use a similarity-weighted aggregation:

$$w_k = \frac{\exp(\text{score}_k/\tau)}{\sum_{u \in \mathcal{N}_{\text{top}}} \exp(\text{score}_u/\tau)}, \quad \mu_{\text{prior}}^c = \sum_{k \in \mathcal{N}_{\text{top}}} w_k \mu_k, \quad (7)$$

where τ is a temperature.

MAP view with spherical uncertainties. We interpret the support prototype p_{init}^c as a noisy observation of the true class mean μ^c under a spherical Gaussian likelihood $p_{\text{init}}^c \sim \mathcal{N}(\mu^c, \sigma_{\text{like}}^2 \mathbf{I})$, while the retrieved prior mean provides a spherical Gaussian prior $p(\mu^c) = \mathcal{N}(\mu_{\text{prior}}^c, \sigma_{\text{prior}}^2 \mathbf{I})$. Under Gaussian–Gaussian conjugacy, the MAP estimate has a closed form that reduces to a convex combination:

$$\tilde{p}^c = \alpha p_{\text{init}}^c + (1 - \alpha) \mu_{\text{prior}}^c, \quad \alpha = \frac{\sigma_{\text{prior}}^2}{\sigma_{\text{prior}}^2 + \sigma_{\text{like}}^2}. \quad (8)$$

Thus, α is determined by the relative confidence between the support evidence and the retrieved semantic prior. In practice, we use a fixed (or learnable) scalar α for efficiency, which is consistent with the above MAP interpretation. Substituting Eq. (7) into Eq. (8) yields the MAP-calibrated prototype \tilde{p}^c for class c . Compared with [Wu *et al.*, 2021; Wu and Hu, 2022], prior selection in PMCE is driven by CLIP-based class-name semantics rather than by visual distances or hand-crafted rules.

4.2 Caption-Guided Dual-Stream Enhancement

We refine representations with instance-level captions by applying the same enhancer Φ to the support and query streams. Given a visual feature and its caption-derived semantic representation, Φ outputs an enhanced visual embedding used for prototype construction and query matching.

Instance-level semantics. To provide finer-grained cues and cover unlabeled queries, we use image captions as instance-level semantics. For any image x , we first generate a caption with a frozen BLIP captioner,

$$c = \text{BLIP}(x), \quad (9)$$

and then encode it with the same text encoder $g_\phi(\cdot)$ to obtain a single sentence embedding:

$$s_{\text{inst}} = g_\phi(c) \in \mathbb{R}^{d_t}, \quad (10)$$

where d_t is the text feature dimension. s_{inst} is label-free and thus available for both supports and queries, serving as the semantic input to Φ on the two streams.

Enhancement module. We define a mapping

$$\mathbf{v}_{\text{out}} = \Phi(\mathbf{v}_{\text{in}}, \mathbf{S}_{\text{in}}; \Theta), \quad (11)$$

where $\mathbf{v}_{\text{in}} \in \mathbb{R}^{1 \times d_v}$ is a visual anchor (e.g., a prototype or a query feature), $\mathbf{S}_{\text{in}} \in \mathbb{R}^{d_t}$ is a semantic context, and Θ are learnable parameters. Since visual and textual features live in different spaces, we first project each semantic token to the visual dimension:

$$\mathbf{S}_{\text{proj}} = \text{ReLU}(\text{LN}(\mathbf{S}_{\text{in}} W_p + b_p)) \in \mathbb{R}^{d_v}, \quad (12)$$

with $W_p \in \mathbb{R}^{d_t \times d_v}$, $b_p \in \mathbb{R}^{d_v}$ and $\text{LN}(\cdot)$ layer normalization.

We then perform cross-attention by using the visual anchor as the query and the caption tokens as keys/values:

$$\mathbf{Q}_{\text{att}} = \mathbf{v}_{\text{in}} W_Q, \quad \mathbf{K}_{\text{att}} = \mathbf{S}_{\text{proj}} W_K, \quad \mathbf{V}_{\text{att}} = \mathbf{S}_{\text{proj}} W_V, \quad (13)$$

where $W_Q, W_K, W_V \in \mathbb{R}^{d_v \times d_k}$ are learnable projections. The attention output is computed as

$$\text{Attn}(\mathbf{Q}_{\text{att}}, \mathbf{K}_{\text{att}}, \mathbf{V}_{\text{att}}) = \text{Softmax}\left(\frac{\mathbf{Q}_{\text{att}} \mathbf{K}_{\text{att}}^\top}{\sqrt{d_k}}\right) \mathbf{V}_{\text{att}}. \quad (14)$$

A residual connection with a learnable scale β (initialized to a small value) preserves the original visual structure:

$$\mathbf{v}_{\text{out}} = \mathbf{v}_{\text{in}} + \beta \text{Attn}(\mathbf{Q}_{\text{att}}, \mathbf{K}_{\text{att}}, \mathbf{V}_{\text{att}}). \quad (15)$$

Support and query streams. We apply $\Phi(\cdot)$ symmetrically to supports and queries. For class c , let \mathcal{S}_c be its support set and $\mathbf{S}_{\text{inst}}^{(i)}$ be the caption embedding of support $x_i \in \mathcal{S}_c$. We average support caption embeddings to form a class-level semantic context:

$$s_{\text{proto}}^c = \frac{1}{|\mathcal{S}_c|} \sum_{x_i \in \mathcal{S}_c} s_{\text{inst}}^{(i)} \in \mathbb{R}^{d_t}. \quad (16)$$

We then take the MAP-calibrated prototype \tilde{p}^c as the visual anchor to obtain the final enhanced prototype:

$$\mathbf{P}_{\text{final}}^c = \Phi(\tilde{p}^c, \mathbf{S}_{\text{proto}}^c). \quad (17)$$

For a query image x_q with visual feature $\mathbf{z}_q = f_\theta(x_q)$ and its caption embedding $\mathbf{S}_{\text{inst}}^q$, we compute

$$\mathbf{Z}_{\text{final}}^q = \Phi(\mathbf{z}_q, \mathbf{S}_{\text{inst}}^q). \quad (18)$$

Each query is processed independently, so the overall framework remains strictly inductive.

4.3 Training Objective with Consistency Regularization

We freeze f_θ and g_ϕ and train only the enhancer Φ together with an auxiliary classifier on base classes. Let $v_{\text{out}}^{(i)}$ be the enhanced feature of a training sample x_i with label y_i .

Classification and prototype-preserving regularization. We use a standard cross-entropy loss

$$\mathcal{L}_{\text{cls}} = -\frac{1}{B} \sum_{i=1}^B \log P(y_i | v_{\text{out}}^{(i)}), \quad (19)$$

Table 1: Comparison with state-of-the-art few-shot learning methods under the 5-way 1-shot and 5-way 5-shot settings on MiniImageNet and TieredImageNet. All results are reported as mean accuracy (%) with 95% confidence intervals. The best performance in each column is highlighted in bold, and “–” indicates that the result is not reported.

Methods	Backbone	Semantic	MiniImageNet		TieredImageNet	
			1-shot	5-shot	1-shot	5-shot
Metric-based						
MatchNet [Vinyals <i>et al.</i> , 2016]	ResNet-12	No	65.64 \pm 0.20	78.72 \pm 0.15	68.50 \pm 0.92	80.60 \pm 0.71
ProtoNet [Snell <i>et al.</i> , 2017]	ResNet-12	No	60.37 \pm 0.83	78.02 \pm 0.57	53.31 \pm 0.89	72.69 \pm 0.74
RelationNet [Sung <i>et al.</i> , 2018]	ConvNet64	No	52.19 \pm 0.83	70.20 \pm 0.66	54.48 \pm 0.93	71.32 \pm 0.78
SeFeat [Afrasiyabi <i>et al.</i> , 2022]	ResNet-12	No	68.32 \pm 0.62	82.71 \pm 0.46	73.63 \pm 0.88	87.59 \pm 0.57
FGFL [Cheng <i>et al.</i> , 2023]	ResNet-12	No	69.14 \pm 0.80	86.01 \pm 0.62	73.21 \pm 0.88	87.21 \pm 0.61
CPEA [Hao <i>et al.</i> , 2023]	ViT-S	No	71.97 \pm 0.65	87.06 \pm 0.38	76.93 \pm 0.70	90.12 \pm 0.45
MCNet [Chen <i>et al.</i> , 2024]	ResNet-18	No	72.13 \pm 0.43	88.20 \pm 0.23	73.14 \pm 0.46	87.16 \pm 0.32
Cads [Zhang <i>et al.</i> , 2025]	ResNet-12	No	66.56 \pm 0.19	82.74 \pm 0.13	72.04 \pm 0.22	86.47 \pm 0.15
SRE-ProtoNet* [Chen <i>et al.</i> , 2025b]	ResNet-12	No	70.86 \pm 0.44	87.01 \pm 0.27	73.02 \pm 0.50	87.78 \pm 0.31
Distribution-based						
ImprovedMAP [Wu and Hu, 2022]	WRN-28-10	Yes	71.56 \pm 0.74	85.05 \pm 0.49	79.26 \pm 0.08	90.41 \pm 0.72
TDO [Liu <i>et al.</i> , 2023]	WRN-28-10	No	74.10 \pm 0.23	86.44 \pm 0.13	82.68 \pm 0.22	90.85 \pm 0.13
PBML [Fu <i>et al.</i> , 2025]	NesT ViT	No	70.04 \pm 0.67	85.21 \pm 0.58	76.73 \pm 0.88	90.11 \pm 0.65
DDC [Chen <i>et al.</i> , 2025a]	WRN-28-10	No	69.17 \pm 1.25	85.23 \pm 0.97	–	–
Semantic-based						
KTN [Peng <i>et al.</i> , 2019]	ConvNet	Yes	64.42 \pm 0.72	74.16 \pm 0.56	63.43 \pm 0.21	74.32 \pm 0.58
AM3 [Xing <i>et al.</i> , 2019]	ResNet-12	Yes	65.30 \pm 0.49	78.10 \pm 0.36	69.08 \pm 0.47	82.58 \pm 0.31
SEGA [Yang <i>et al.</i> , 2022a]	ResNet-12	Yes	69.04 \pm 0.26	79.03 \pm 0.18	72.18 \pm 0.30	84.28 \pm 0.21
BMI [Li and Wang, 2023]	ResNet-12	Yes	77.01 \pm 0.34	84.85 \pm 0.27	78.37 \pm 0.44	86.30 \pm 0.32
MAVSI [Zhao <i>et al.</i> , 2024]	ResNet-12	Yes	69.74 \pm 0.21	82.23 \pm 0.41	74.61 \pm 0.18	87.45 \pm 0.46
SEVPro [Cai <i>et al.</i> , 2024a]	ResNet-12	Yes	71.81 \pm 0.22	78.88 \pm 0.18	72.77 \pm 0.30	84.04 \pm 0.21
PRSN [Dong <i>et al.</i> , 2025]	ResNet-12	Yes	71.09 \pm 0.90	86.82 \pm 0.61	74.14 \pm 0.86	88.54 \pm 0.61
Vision-language based						
SP-CLIP [Chen <i>et al.</i> , 2023b]	ViT-T	Yes	72.31 \pm 0.40	83.42 \pm 0.30	78.03 \pm 0.46	88.55 \pm 0.32
SP-SBERT [Chen <i>et al.</i> , 2023b]	ViT-T	Yes	70.70 \pm 0.42	83.55 \pm 0.30	73.31 \pm 0.50	88.56 \pm 0.32
SP-Glove [Chen <i>et al.</i> , 2023b]	ViT-T	Yes	70.81 \pm 0.42	83.31 \pm 0.30	74.68 \pm 0.50	88.64 \pm 0.31
SemFew-Trans [Zhang <i>et al.</i> , 2024a]	Swin-T	Yes	78.94 \pm 0.66	86.49 \pm 0.50	82.37 \pm 0.77	89.89 \pm 0.52
SYNTRANS [Tang <i>et al.</i> , 2025]	ResNet-12	Yes	76.20 \pm 0.69	86.12 \pm 0.54	79.69 \pm 0.81	87.78 \pm 0.60
PMCE(Ours)	ResNet-12	Yes	82.90 \pm 0.78	92.29 \pm 0.46	83.50 \pm 0.32	95.03 \pm 0.34
	Swin-T	Yes	85.03 \pm 0.67	92.77 \pm 0.37	83.13 \pm 0.33	93.23 \pm 0.43

and a lightweight prototype-preserving term that discourages excessive drift from the frozen backbone structure:

$$\mathcal{L}_{\text{rec}} = \frac{1}{B} \sum_{i=1}^B \|v_{\text{out}}^{(i)} - \mu_{\text{proto}}^{y_i}\|_1. \quad (20)$$

We use a small λ_{rec} so that the enhancer can still introduce caption-guided adaptation while keeping base-class geometry stable.

Caption consistency with supervised contrastive learning. Caption quality may vary, so we add a consistency regularization on caption semantics in the projected space. For sample x_i , let $s_{\text{proj}}^{(i)} \in \mathbb{R}^{d_v}$ be the projected caption embedding (Eq. (12)). We normalize it as

$$v_i^{\text{cap}} = \frac{s_{\text{proj}}^{(i)}}{\|s_{\text{proj}}^{(i)}\|} \in \mathbb{R}^{d_v}. \quad (21)$$

We encourage captions from the same class to be coherent while maintaining inter-class separation via a supervised con-

trastive loss:

$$\mathcal{L}_{\text{con}} = \frac{1}{B} \sum_{i=1}^B \left[-\frac{1}{|\mathcal{P}(i)|} \sum_{p \in \mathcal{P}(i)} \log \frac{\exp(\cos(v_i^{\text{cap}}, v_p^{\text{cap}})/\tau_c)}{\sum_{\substack{a=1 \\ a \neq i}}^B \exp(\cos(v_i^{\text{cap}}, v_a^{\text{cap}})/\tau_c)} \right], \quad (22)$$

where $\mathcal{P}(i) = \{p \neq i \mid y_p = y_i\}$ denotes positives in the mini-batch and τ_c is a temperature.

Overall objective. The final objective is

$$\mathcal{L}_{\text{total}} = \mathcal{L}_{\text{cls}} + \lambda_{\text{rec}} \mathcal{L}_{\text{rec}} + \lambda_{\text{con}} \mathcal{L}_{\text{con}}, \quad (23)$$

with λ_{rec} and λ_{con} tuned on the validation set. During meta-test, f_θ , g_ϕ and Φ are all frozen, and classification is performed with logistic regression using enhanced support and query features.

5 Experiments

Datasets. We evaluate PMCE on four standard few-shot benchmarks, including MiniImageNet, TieredImageNet, CIFAR-FS, and FC100. MiniImageNet [Vinyals *et al.*, 2016]

Table 2: Comparison with state-of-the-art few-shot learning methods under the 5-way 1-shot and 5-way 5-shot settings on CIFAR-FS and FC100. All results are reported as mean accuracy (%) with 95% confidence intervals. The best performance in each column is highlighted in bold, and “–” indicates that the result is not reported.

Methods	Backbone	Semantic	CIFAR-FS		FC100	
			1-shot	5-shot	1-shot	5-shot
Metric-based						
ProtoNet [Snell <i>et al.</i> , 2017]	ResNet-12	No	55.50 \pm 0.70	72.00 \pm 0.60	41.54 \pm 0.76	57.08 \pm 0.76
MetaOptNet [Lee <i>et al.</i> , 2019]	ResNet-12	No	72.80 \pm 0.70	84.30 \pm 0.50	47.20 \pm 0.60	55.50 \pm 0.60
CORL [He <i>et al.</i> , 2023]	ResNet-12	No	74.13 \pm 0.71	87.54 \pm 0.51	44.82 \pm 0.73	61.31 \pm 0.54
QSFormer [Wang <i>et al.</i> , 2023b]	ResNet-12	No	46.51 \pm 0.26	61.58 \pm 0.25	–	–
SSFormers [Chen <i>et al.</i> , 2023a]	ResNet-12	No	74.50 \pm 0.21	86.61 \pm 0.23	43.72 \pm 0.21	58.92 \pm 0.18
Cads [Zhang <i>et al.</i> , 2025]	ResNet-12	No	73.23 \pm 0.21	87.67 \pm 0.14	–	–
Distribution-based						
PBML [Fu <i>et al.</i> , 2025]	ResNet-12	No	73.07 \pm 0.59	85.51 \pm 0.41	47.92 \pm 0.49	62.96 \pm 0.51
DDC [Chen <i>et al.</i> , 2025a]	WRN-28-10	No	76.47 \pm 1.86	87.24 \pm 0.89	–	–
Semantic-based						
ProtoNet + SEVPro [Cai <i>et al.</i> , 2024b]	ResNet-12	Yes	74.01 \pm 0.29	85.86 \pm 0.20	–	–
PRSN [Dong <i>et al.</i> , 2025]	ResNet-12	Yes	78.72 \pm 0.96	90.22 \pm 0.60	47.91 \pm 0.57	62.95 \pm 0.52
Vision-language based						
LPE [Yang <i>et al.</i> , 2023]	ResNet-12	Yes	74.88 \pm 0.45	85.30 \pm 0.35	–	–
SP-Pretrain [Chen <i>et al.</i> , 2023b]	ViT-S	Yes	71.99 \pm 0.47	85.98 \pm 0.34	43.77 \pm 0.39	59.48 \pm 0.39
SAFF [Cumplido <i>et al.</i> , 2025]	Vit-B	Yes	78.50 \pm 0.30	90.26 \pm 0.08	47.17 \pm 0.12	66.22 \pm 0.51
PMCE(Ours)	ResNet-12	Yes	76.97 \pm 0.81	84.76 \pm 0.61	49.81 \pm 0.82	63.67 \pm 0.73
	Swin-T	Yes	80.92 \pm 0.72	89.02 \pm 0.58	52.46 \pm 0.82	67.00 \pm 0.75

and TieredImageNet [Ren *et al.*, 2018] are subsets of ImageNet [Russakovsky *et al.*, 2015] with 64, 16, and 20 classes for base, validation, and novel splits, and 351, 97, and 160 classes for base, validation, and novel splits, respectively. CIFAR-FS [Bertinetto *et al.*, 2019] follows a random split of CIFAR-100 into 64, 16, and 20 classes, while FC100 [Oreshkin *et al.*, 2018] adopts a superclass-based split with 60, 20, and 20 classes to reduce semantic overlap between base and novel categories.

Implementation details. Following [Zhao *et al.*, 2024], we use ResNet-12 [He *et al.*, 2016] and Swin-T [Liu *et al.*, 2021] as visual backbones. Captions are generated using a frozen BLIP captioner, and both class names and captions are encoded by ViT-B/16 CLIP [Radford *et al.*, 2021] into 512-dimensional semantic features. All CLIP and BLIP components remain frozen throughout training and evaluation. The enhancer Φ consists of a projection layer with Linear, LayerNorm, and ReLU, followed by multi-head attention, with a residual update scaled by a learnable factor β initialized to 0.1. We use $h = 4$ heads and dropout 0; the key dimension is $d_k = 160$ for ResNet-12 ($d_v = 640$) and $d_k = 192$ for Swin-T ($d_v = 768$). All backbones and BLIP/CLIP modules remain frozen, and inference is strictly inductive.

We follow a two-stage training protocol. We load the backbone pre-trained in [Zhao *et al.*, 2024], freeze it, and train only Φ together with an auxiliary classifier for 50 epochs using Adam with learning rate 10^{-4} and batch size 128. During evaluation, we sample 600 episodes for each 5-way 1-shot and 5-way 5-shot setting and report mean accuracy with 95% confidence intervals; logistic regression is used by default, and nearest-prototype yields similar trends. Unless otherwise specified, we set $\alpha = 0.33$ for 1-shot and $\alpha = 0.7$ for 5-shot in Eq. (3), use top- k retrieval with $k = 7$ and

Table 3: Ablation of PMCE components under the 5-way 1-shot setting on MiniImageNet and FC100 with the Swin-T backbone. MAP denotes semantics-guided prior calibration; Enh.(S) and Enh.(Q) denote caption-guided enhancement on the support and query streams. We report mean accuracy (%) \pm 95% confidence intervals.

MAP	Enh.(S)	Enh.(Q)	MiniImageNet	FC100
×	×	×	71.02 \pm 0.79	45.27 \pm 0.75
×	✓	×	72.18 \pm 0.78	46.03 \pm 0.74
×	✗	✓	72.49 \pm 0.81	45.47 \pm 0.77
✓	✗	✗	74.93 \pm 0.76	45.36 \pm 0.75
✓	✓	✗	74.99 \pm 0.74	45.15 \pm 0.77
✓	✗	✓	77.17 \pm 0.76	45.27 \pm 0.78
✗	✓	✓	79.42 \pm 0.73	48.79 \pm 0.80
✓	✓	✓	85.03 \pm 0.67	52.46 \pm 0.82

temperature $\tau = 1.0$, and set $\tau_c = 0.1$, $\lambda_{\text{rec}} = 1.0$, and $\lambda_{\text{con}} = 1.0$ for training. We use class-name embeddings for retrieval since they are stable and class-consistent, while captions can be noisier on low-resolution images. We also experimented with token-level caption features, but they lead to significantly larger intermediate files and storage overhead, so we report sentence-embedding results by default.

5.1 Experimental Results

We compare PMCE with representative metric-based methods FGFL [Cheng *et al.*, 2023] and CPEA [Hao *et al.*, 2023], distribution-based methods MAP [Wu *et al.*, 2021] and ImprovedMAP [Wu and Hu, 2022], and recent semantic and vision-language baselines BMI [Li and Wang, 2023], SP-CLIP [Chen *et al.*, 2023b], SemFew-Trans [Zhang *et al.*, 2024a], and PRSN [Dong *et al.*, 2025]. Results on MiniImageNet and TieredImageNet are reported in Tab. 1, and results

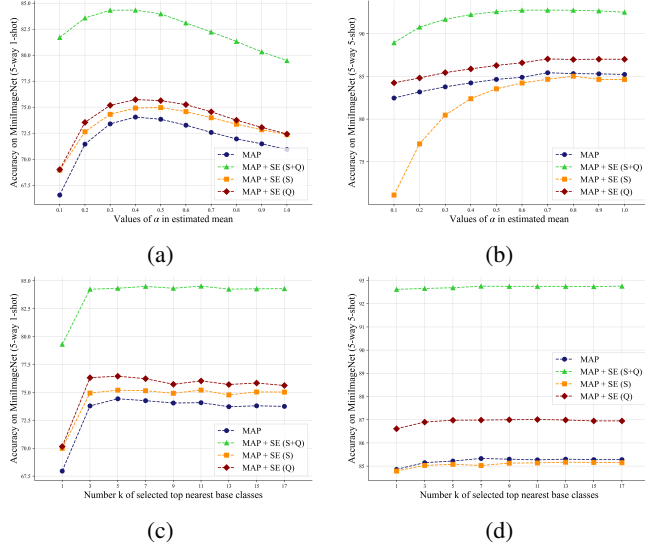


Figure 3: Sensitivity of PMCE to the prior weight α and the number of retrieved base classes k on MiniImageNet. Performance is stable over a wide range of values, and our default settings lie in the high-accuracy region.

on CIFAR-FS and FC100 are reported in Tab. 2.

Across ImageNet-style benchmarks, PMCE consistently improves over strong semantic and vision–language baselines under both ResNet-12 and Swin-T. The gains are most apparent in the 1-shot regime, where prototype bias is severe and query-side refinement becomes critical. For example, as is shown in Tab. 1, with Swin-T, PMCE reaches 85.03% on MiniImageNet 1-shot and surpasses SemFew-Trans [Zhang *et al.*, 2024a] by 7.71% in this setting. Similar improvements are observed on TieredImageNet, indicating that the benefit transfers to a larger and more diverse label space.

On CIFAR-100 derived benchmarks, the 32×32 resolution makes captions less specific, which naturally attenuates the advantage of instance-level semantics. Nevertheless, as shown in Tab. 2, PMCE remains competitive on CIFAR-FS and achieves the best 1-shot accuracy of 80.92%, surpassing PRSN by 2.79%. On FC100, PMCE achieves the top performance with 52.46% and 67.00%, yielding improvements over PRSN by 9.5% and 6.43%, respectively.

Overall, PMCE delivers consistent gains across backbones, with the most stable improvements on ImageNet-style benchmarks where captions are more informative. We believe the improvements mainly come from two design choices. First, semantics-guided prior retrieval provides a class-specific prior that stabilizes prototype estimation when supports are extremely limited, which is especially important in 1-shot. Second, PMCE optimizes the query side with label-free captions under the inductive protocol, so support and query features are better aligned before matching.

5.2 Empirical Analysis

Ablation study. Tab. 3 analyzes key components under the 5-way 1-shot setting on MiniImageNet and FC100 with the Swin-T backbone. The baseline achieves 71.02% on Mini-

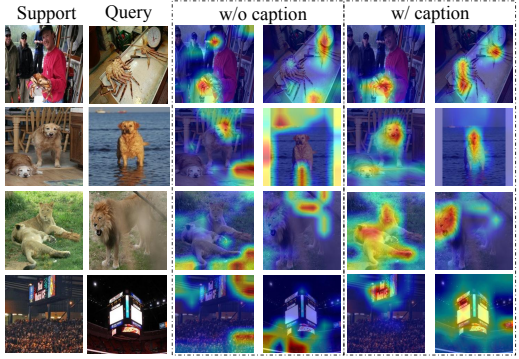


Figure 4: Grad-CAM visualizations on the MiniImageNet test set. Compared with **w/o caption**, **w/ caption** produces more focused activations on query images, suppressing background responses and highlighting discriminative object regions.

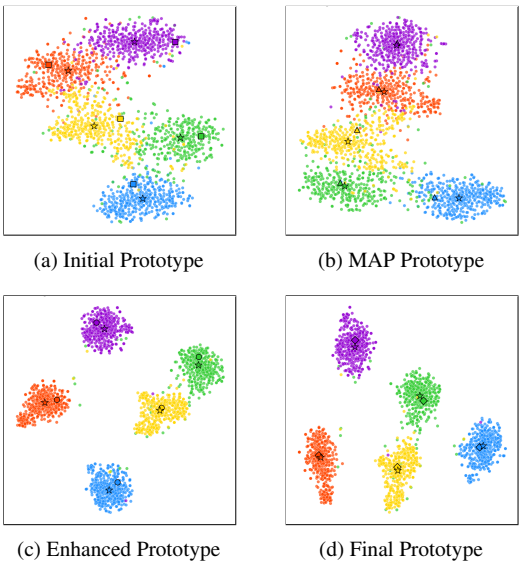


Figure 5: t-SNE visualization of feature distributions and prototype evolution on a 5-way 1-shot task from MiniImageNet. Different colors denote classes; \star are ground-truth centers, \blacksquare initial prototypes, \triangle MAP rectified prototypes, large \bullet caption-enhanced prototypes, and \diamond the final prototypes of PMCE. MAP calibration and caption-guided enhancement jointly move prototypes toward the true centers and make clusters more compact.

ImageNet and 45.27% on FC100. Adding semantics-guided MAP calibration alone improves MiniImageNet to 74.93%, which corresponds to a gain of 5.51%. Applying caption-guided enhancement to a single stream yields smaller gains, and query-side enhancement is more influential than support-side enhancement. Enhancing both streams without MAP reaches 79.42% on MiniImageNet and 48.79% on FC100. Combining MAP calibration with dual-stream enhancement yields the best performance, reaching 85.03% on MiniImageNet and 52.46% on FC100, which improves over the baseline by 19.73% and 15.88%.

Impact of hyperparameters. Fig. 3 explores the prior weight α in Eq. (3) and the neighbor count k assigned for

prior retrieval. In 1-shot, the high-accuracy region concentrates around α in the range of 0.3 to 0.4. In 5-shot, the best region shifts toward a larger α around 0.7. Accuracy remains stable across a wide range of k , indicating that the retrieval step is not critically dependent on the precise count of base classes.

5.3 Visualization Analysis

Effect of caption guidance. Fig. 4 compares Grad-CAM activation maps with and without caption guidance. Without captions, query responses are often diffuse and may include background regions. With caption guidance, activations become more concentrated on object regions and less affected by background clutter.

Prototype evolution. Fig. 5 visualizes feature distributions and prototype evolution on a 5-way 1-shot episode from MiniImageNet. MAP calibration shifts prototypes toward more reasonable regions by injecting class-specific priors, and caption-guided enhancement further tightens clusters and improves inter-class separation. The final prototypes are closer to the ground-truth centers, supporting that PMCE improves prototype estimation and query-side representations in a unified metric space.

6 Conclusion

In this paper, we have presented PMCE, a probabilistic few-shot framework that integrates semantics-guided prior selection, MAP prototype calibration, and caption-guided feature optimization. By using class-name embeddings to select class-specific priors from base statistics and leveraging BLIP captions as label-free instance cues for both supports and queries, PMCE produces more stable prototypes and better-aligned query representations, with a lightweight consistency regularizer to mitigate caption noise. Experiments on four benchmarks with two backbones show consistent improvements over strong metric-, semantic-, and distribution-based baselines, with the most pronounced gains in the 1-shot setting. Future work will explore the confidence of captions to further reduce semantic drift under noisy semantics.

A Appendix

A.1 Additional Implementation Details for PMCE

To ensure the reproducibility of our PMCE framework, we provide the detailed algorithmic procedures for the two core components: Semantics-Guided Prior Selection and Caption-Guided Feature Enhancement.

Semantics-guided MAP Prototype Calibration

Algorithm 1 details how we rectify support prototypes by leveraging priors from the base classes.

Algorithmic Steps. Our procedure begins by retrieving the top- K semantically similar base classes. We then aggregate their visual means to form μ_{prior} . This prior is then fused with the support prototype p_{init} to compute the calibrated prototype \tilde{p} . The hyperparameter α is employed to balance the contribution between the support information and the retrieved base-class knowledge across different shot settings.

Algorithm 1 Semantics-guided MAP Prototype Calibration (Weighted Prior)

Input: Support set \mathcal{S} , novel class semantic s_{class} , Knowledge Bank $\mathcal{B} = \{(\mu_j, s_{base}^j)\}_{j=1}^{|\mathcal{C}_b|}$

Parameter: Number of neighbors K , balancing hyperparameter α , temperature τ

Output: Rectified prototype \tilde{p}

- 1: Compute the empirical prototype p_{init} by averaging features of \mathcal{S} .
- 2: **for** each base class $(\mu_j, s_{base}^j) \in \mathcal{B}$ **do**
- 3: Calculate semantic similarity score $_j = \cos(s_{class}, s_{base}^j)$ according to Eq. (3).
- 4: **end for**
- 5: Select Top- K indices to form the neighbor set \mathcal{N}_{top} .
- 6: Compute normalized weights $w_k = \frac{\exp(score_k/\tau)}{\sum_{u \in \mathcal{N}_{top}} \exp(score_u/\tau)}$, $\forall k \in \mathcal{N}_{top}$.
- 7: Aggregate visual priors: $\mu_{prior} = \sum_{k \in \mathcal{N}_{top}} w_k \mu_k$.
- 8: Calculate $\tilde{p} = \alpha p_{init} + (1 - \alpha) \mu_{prior}$ following Eq. (6).
- 9: **return** \tilde{p}

Algorithm 2 Forward Pass of the Caption-Guided Enhancer Φ

Input: Visual feature $v_{in} \in \mathbb{R}^{1 \times d_v}$, caption embedding $\mathbf{S}_{in} \in \mathbb{R}^{d_v}$

Parameter: Projection layer $(W_p, b_p, LN, ReLU)$, multi-head cross-attention Attn (heads h), projections (W_Q, W_K, W_V) , scaling factor β

Output: Enhanced feature v_{out}

- 1: **Semantic Projection (token-wise):** $\mathbf{S}_{proj} \leftarrow ReLU(LN(\mathbf{S}_{in}W_p + b_p)) \in \mathbb{R}^{d_v}$.
- 2: **Cross-Attention (visual token \rightarrow caption tokens):** $\mathbf{Q} \leftarrow v_{in}W_Q \in \mathbb{R}^{1 \times d_k}$, $\mathbf{K} \leftarrow \mathbf{S}_{proj}W_K \in \mathbb{R}^{1 \times d_k}$, $\mathbf{V} \leftarrow \mathbf{S}_{proj}W_V \in \mathbb{R}^{1 \times d_k}$.
- 3: Compute attention map: $\mathbf{A} \leftarrow \text{Softmax}(\frac{\mathbf{Q}\mathbf{K}^\top}{\sqrt{d_k}}) \in \mathbb{R}^{1 \times T}$.
- 4: Obtain attended semantic residual: $\Delta v \leftarrow \mathbf{A}\mathbf{V} \in \mathbb{R}^{1 \times d_k}$.
- 5: (Multi-head) Apply the above per head and concatenate/project to match d_v (standard MHA).
- 6: **Residual Integration:** $v_{out} \leftarrow v_{in} + \beta \cdot \Delta v$.
- 7: **return** v_{out}

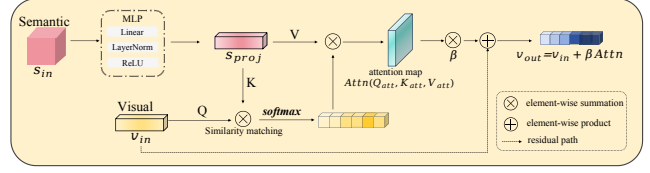


Figure 6: Architecture of the caption-guided enhancer Φ . Instance-level semantics from captions are projected and injected into visual features via cross-attention, and a learnable factor β controls the strength of the semantic residual.

Details of the Caption-Guided Enhancer Module

To supplement the methodology in Section 4.2, we provide further implementation details of the Caption-Guided Enhancer Φ . Algorithm 2 details the overall execution logic for this process. As illustrated in Figure 6, Φ is designed as a lightweight cross-modal residual block that refines visual representations by leveraging instance-level semantic contexts.

Feature Interaction. Consistent with Eqs. (12)–(15), the module first aligns the caption embedding s_{in} to the visual space via a projection layer: $s_{proj} = \text{ReLU}(\text{LN}(W_p s_{in} + b_p))$. We then model the primary interaction through a multi-head cross-attention mechanism, configuring the number of heads to $h = 4$. Utilizing h attention heads enables the model to capture diverse information from multiple semantic subspaces simultaneously.

Gated Residual Connection. To keep the pre-trained backbone’s discriminative power intact, we integrate the attention output through a gated residual path: $v_{out} = v_{in} + \beta \text{Attn}(Q, K, V)$, following the formulation in Eq. 15. Notably, the learnable scaling factor β is initialized to 0.1. Such an initialization strategy provides an initial momentum for visual-semantic fusion. More importantly, it shields the model from overlooking semantic cues or experiencing unstable gradients as training begins.

A.2 Impact of Classification Strategies and Retrieval Cues

Figure 7 illustrates a comparison between two distinct retrieval strategies. Initially, we use coarse-grained class-name semantics for both the base and support sets. The second uses concatenated class-name and caption semantics for the base set and the averaged caption features of the support samples for the current task. As shown in Fig. 7a, class-name semantics provide more accurate retrieval in the 1-shot setting. In contrast, under the 5-shot setting (Fig. 7b), the difference between the two strategies becomes negligible. Due to its performance in extreme low-data regimes, we adopt the class-name semantics as our default retrieval cue. We further assess the effect of the classifier on the final accuracy. Table 4 presents the results of three classifiers, in which logistic classifier achieves the best overall performance, the margins between the three methods are remarkably narrow.

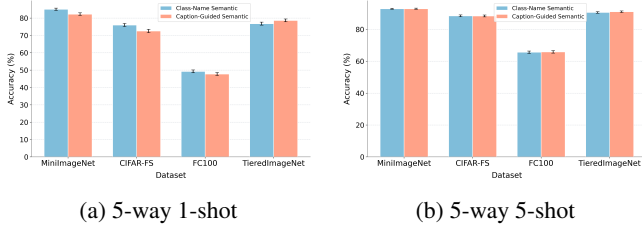


Figure 7: Comparison of different semantic distance cues used for distance-based prior candidate selection in the MAP framework. The semantic information here is used to compute distances for selecting relevant base-class statistics in MAP, rather than being directly modeled as a probabilistic prior or used for feature enhancement.

Table 4: Average classification accuracy (%) of different classifiers under the same MAP framework. All results are reported using a fixed semantic distance cue for distance-based prior candidate selection in MAP. LR denotes the linear logistic regression classifier, EU denotes the Euclidean-distance nearest-prototype classifier, and CO denotes the cosine-distance nearest-prototype classifier.

Classifier	MiniImageNet		TieredImageNet		CIFAR-FS		FC100	
	1-shot	5-shot	1-shot	5-shot	1-shot	5-shot	1-shot	5-shot
EU	83.84	92.59	82.04	93.07	79.44	88.30	52.01	67.16
CO	83.83	92.60	82.91	93.08	79.48	88.19	52.28	66.98
LR	85.03	92.77	83.13	93.23	80.92	89.02	52.46	67.00

Table 5: The 5-way 1-shot and 5-way 5-shot accuracy (%) for cross-domain on MiniImageNet → CUB. The best results are highlighted in bold.

Method	Semantic	MiniImageNet → CUB	
		5-way 1-shot	5-way 5-shot
MatchNet [Vinyals <i>et al.</i> , 2016]	No	42.62 ± 0.55	56.53 ± 0.44
ProtoNet [Snell <i>et al.</i> , 2017]	No	50.51 ± 0.56	69.28 ± 0.40
MAML [Finn <i>et al.</i> , 2017]	No	43.59 ± 0.54	54.18 ± 0.41
RelationNet [Sung <i>et al.</i> , 2018]	No	49.84 ± 0.54	68.98 ± 0.42
SimpleShot [Wang <i>et al.</i> , 2019]	No	48.56	65.63
GNN + FT [Tseng <i>et al.</i> , 2020]	No	47.47 ± 0.75	66.98 ± 0.68
MN + AFA [Hu and Ma, 2022]	No	41.02	59.46
StyleAdv [Fu <i>et al.</i> , 2023]	No	48.49	68.72
LDP-net [Zhou <i>et al.</i> , 2023]	No	49.82	70.39
MIFN [Zhou <i>et al.</i> , 2023]	Yes	48.21 ± 0.60	65.33 ± 0.54
MIFN+Ltri [Zhou <i>et al.</i> , 2023]	Yes	49.21 ± 0.60	66.30 ± 0.56
FLoR [Zou <i>et al.</i> , 2024]	No	49.99	70.39
TPN-FAP [Zhang <i>et al.</i> , 2024b]	Yes	50.56 ± 0.50	64.17 ± 0.40
TA-MLA [Yue <i>et al.</i> , 2025]	Yes	48.57 ± 0.47	69.92 ± 0.45
PMCE (ours)	Yes	52.09 ± 0.88	70.79 ± 0.78

A.3 Evaluation on Cross-Domain Adaptation

To assess the cross-domain generalization of PMCE, we further evaluate it in the cross-domain few-shot setting, where episodes are sampled from a target dataset with a distribution different from the base training data. The quantitative results are reported in Tab. 5. Overall, PMCE attains accuracy comparable to recent strong baselines under this challenging protocol. In the 5-way 5-shot case, it slightly surpasses the metric-based LDP-Net by 0.40%, while remaining on par with it in the 1-shot setting.

These results indicate that the proposed caption-guided enhancement can still provide useful auxiliary cues when there is a noticeable domain gap, although the absolute accuracies are naturally lower than in the in-domain scenario. Semantic cross-attention thus offers a modest but consistent benefit for cross-domain generalization, especially when a few more labeled examples are available.

A.4 BLIP Pre-training and Potential Data Overlap

We use the *blip-image-captioning-base* model to generate instance-level captions. This captioner is pre-trained for image–text generation on a mixture of human-annotated datasets (COCO [Lin *et al.*, 2014], Visual Genome [Krishna *et al.*, 2017]) and web-scale collections (Conceptual Captions and Conceptual 12M [Changpinyo *et al.*, 2021], SBU captions [Ordonez *et al.*, 2011], LAION [Schuhmann *et al.*, 2021]). In our few-shot pipeline, BLIP is kept frozen and is only applied to images from the base and novel sets, similar to a fixed visual backbone. The model is trained for caption generation rather than classification, and we do not fine-tune it on any of the few-shot benchmarks (MiniImageNet, TieredImageNet, CIFAR-FS, FC100). Although some overlap between web-scale pre-training corpora and benchmark images cannot be completely ruled out, any such overlap is indirect and does not reuse class labels. Conceptually, this setting is analogous to using an ImageNet- or CLIP-pretrained encoder as a frozen feature extractor, and the improvements of PMCE mainly come from how captions are used as label-free semantic cues within an inductive protocol rather than from task-specific pre-training on the target datasets.

In Figure 8, we present several examples from MiniImageNet and CIFAR-FS. Here, ground-truth labels appear above the images while the corresponding BLIP captions are listed below. Instead of reproducing fine-grained class names, the generated captions focus on visible attributes like color, pose, background, and coarse object categories. Taking the “golden retriever” class as an example, the model typically generates descriptions like “a dog lying on the floor with a toy.” Similarly, it identifies a “king crab” simply as “a crab on a black surface”. When handling low-resolution datasets such as CIFAR-FS, BLIP often yields brief, generic phrases. This behavior suggests that the output reflects inherent visual ambiguity rather than a direct retrieval of benchmark labels. Such results reinforce our interpretation of BLIP as a generic visual descriptor here, as opposed to a mere repository for memorized labels.

We kept the BLIP captioner frozen across all experimental phases, including both training and meta-test time. It is applied to support and query images in the same way and is never updated using support sets or query labels. Each query is processed independently, without access to the joint distribution of the query set. Under this setting, captions function as additional instance-level cues injected into an inductive few-shot pipeline, not as an extra supervised signal tuned on the target tasks.

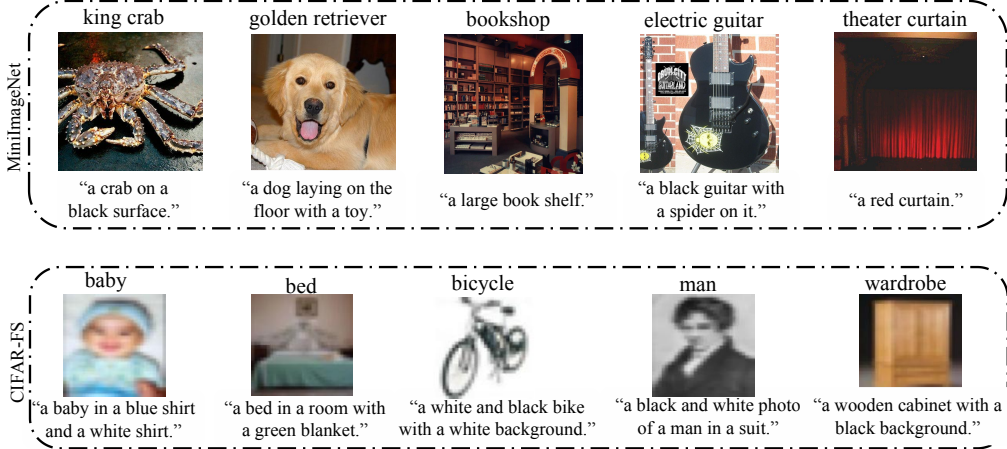


Figure 8: Visualizations of example images from MiniImageNet and CIFAR-FS datasets. For each sample, the category name is displayed above the image, while the generated descriptive caption is provided below.

Table 6: Qualitative comparison between PMCE and recent semantic-driven few-shot methods. We summarize the semantic source, signal granularity and interaction mechanism for each line of work.

Category	Methodology	Semantic Source	Signal Granularity	Interaction Mechanism
Semantic-based (Class-level)	BMI [Li and Wang, 2023]	Category Names (CLIP)	Coarse (Class-level)	Latent space alignment
	MAVSI [Zhao <i>et al.</i> , 2024]	Category Names (GloVe)	Coarse (Class-level)	Multi-attention interaction
	SEVPro [Cai <i>et al.</i> , 2024a]	Category Names (CLIP)	Coarse (Class-level)	Semantic-to-Visual Projection and Prototype Enhancement
	PRSN [Dong <i>et al.</i> , 2025]	Category Names (BERT)	Coarse (Class-level)	Prototype Resynthesis with Cross-image Semantic Alignment
Vision-Language (Class-level)	LPE [Yang <i>et al.</i> , 2023]	Visual Attributes (VLM Embeddings)	Detailed (Class-centric)	Class-specific Part Filters and Latent Embedding
	SP-CLIP [Chen <i>et al.</i> , 2023b]	Category Names (LLM/CLIP)	Static (Class-centric)	Spatial and Channel-wise Prompt Tuning
	SemFew [Zhang <i>et al.</i> , 2024a]	LLM (Evolved descriptions)	Refined (Class-centric)	Semantic Alignment Network
	SYNTRANS [Tang <i>et al.</i> , 2025]	LMMS (CLIP + LLM)	Synergistic (Class-centric)	Synergistic Knowledge Mining and Visual-Semantic Bridging
	SAFF [Cumplido <i>et al.</i> , 2025]	VLM Semantics	Selective (Class-centric)	Slot-based Feature Filtering with Weighted Masking
Ours	VT-FSL [Li <i>et al.</i> , 2025]	LLM-based Iterative Descriptions	Refined (Class-centric)	Cross-modal Geometric Alignment
	PMCE	Category Names (CLIP) Instance Caption (BLIP)	Coarse (Class-level) Dynamic (Instance-level)	Prior selection for MAP-based Calibration Visual-to-semantic cross-attention for instance-level prototype alignment

A.5 Qualitative Comparison with Semantic-Driven FSL

To put PMCE in context, we briefly review recent semantic-driven few-shot methods from the last three years and compare them along three axes: where the semantic signal comes from, at which granularity it is defined, and how heavy the underlying models are and how they are trained. Table 6 summarizes representative approaches.

Semantic-based methods with class-level labels. BMI [Li and Wang, 2023], MAVSI [Zhao *et al.*, 2024], SEVPro [Cai *et al.*, 2024a] and PRSN [Dong *et al.*, 2025] rely on category names or other coarse class-level descriptions as their only semantic source. MAVSI encodes each class name with GloVe and injects these word vectors into the prototype space by multi-head attention. BMI and SEVPro use CLIP text encoders to embed prompts such as “a photo of a {label}” and then adapt visual prototypes or metric heads, while PRSN explores linguistic structures in WordNet or BERT spaces and resynthesizes prototypes via cross-image semantic alignment. Most of these methods attach relatively light semantic modules to a standard few-shot backbone and keep the overall model size comparable to classical metric-based pipelines.

In all cases, every image of a class shares the same semantic vector, which is static once the label is fixed. This

strengthens coarse category alignment but cannot capture fine-grained cues such as pose, background or local texture. When classes are visually similar, for example on FC100, this class-invariant treatment limits how much additional discrimination the semantics can provide.

Vision-language methods with class-level prompts. A second group uses larger language models or vision-language models to enrich class-level semantics before injecting them into the vision pipeline. LPE [Yang *et al.*, 2023] predicts visual attributes with a VLM and uses them as class-specific part filters. SP-CLIP [Chen *et al.*, 2023b] and SemFew [Zhang *et al.*, 2024a] let LLMs refine CLIP prompts into more informative textual descriptions and then tune CLIP with spatial or channel-wise prompts. SYNTRANS [Tang *et al.*, 2025] combines CLIP with an LLM to transfer semantic knowledge to a lighter vision encoder, while SAFF [Cumplido *et al.*, 2025] uses VLM-derived semantics to drive slot-based feature filtering. VT-FSL [Li *et al.*, 2025] iteratively generates class-centric descriptions and aligns them with visual features in a geometric manner.

Compared with the first group, these approaches obtain richer and often more detailed text for each category and sometimes use much heavier backbones or language decoders. Several methods partially fine-tune CLIP or attach learnable adapters and prompt modules with millions of parameters. This improves accuracy but also blurs the line be-

tween gains from semantic design and gains from scaling model capacity and task-specific tuning. Moreover, the semantics are still essentially class-centric: all images from “golden retriever” share one refined description, regardless of the scene or pose, so the semantic branch remains blind to the specific context of each query.

Position of PMCE. PMCE differs from both groups in terms of semantic granularity and model usage. First, class names are not used to directly reshape features or classifier weights. CLIP text embeddings of category names act as keys for retrieving a small set of related base classes, and only their visual statistics enter the MAP-based prior for prototype calibration. Semantics decide which priors are selected, while the priors themselves live in the visual space.

Second, PMCE introduces instance-level captions as a dynamic semantic branch. A frozen BLIP captioner provides a label-free caption for each image, and the caption-guided enhancer uses cross-attention to align these instance-level cues with both support prototypes and query features. As a result, PMCE moves from purely class-level semantics to a mixed granularity where category names govern prior selection and captions adjust feature representations on a per-image basis. This helps the model capture contextual variations inside a class and strengthens discrimination in challenging 1-shot and coarse-grained settings.

Finally, PMCE keeps all large pre-trained components frozen. The visual backbone is a standard ResNet-12 or Swin-T, and the only trainable parts are a lightweight enhancer and an auxiliary classifier on base classes. Unlike recent works that fine-tune CLIP or pair FSL with very large VLM/LLM backbones, our improvements mainly stem from how semantics are used to select priors and reshape prototypes rather than from scaling model size. This makes PMCE complementary to large-model pipelines and also easier to deploy in resource-constrained scenarios.

References

[Afrasiyabi *et al.*, 2022] Arman Afrasiyabi, Hugo Larochelle, Jean-François Lalonde, and Christian Gagné. Matching feature sets for few-shot image classification. In *IEEE/CVF Conference on Computer Vision and Pattern Recognition, CVPR 2022, New Orleans, LA, USA, June 18-24, 2022*, pages 9004–9014. IEEE, 2022.

[Bertinetto *et al.*, 2019] Luca Bertinetto, João F. Henriques, Philip H. S. Torr, and Andrea Vedaldi. Meta-learning with differentiable closed-form solvers. In *7th International Conference on Learning Representations, ICLR 2019, New Orleans, LA, USA, May 6-9, 2019*. OpenReview.net, 2019.

[Cai *et al.*, 2024a] Hecheng Cai, Yang Liu, Shudong Huang, and Jiancheng Lv. With a little help from language: Semantic enhanced visual prototype framework for few-shot learning. In *Proceedings of the Thirty-Third International Joint Conference on Artificial Intelligence, IJCAI 2024, Jeju, South Korea, August 3-9, 2024*, pages 3751–3759. ijcai.org, 2024.

[Cai *et al.*, 2024b] Hecheng Cai, Yang Liu, Shudong Huang, and Jiancheng Lv. With a little help from language: Semantic enhanced visual prototype framework for few-shot learning. In *Proceedings of the Thirty-Third International Joint Conference on Artificial Intelligence, IJCAI 2024, Jeju, South Korea, August 3-9, 2024*, pages 3751–3759. ijcai.org, 2024.

[Changpinyo *et al.*, 2021] Soravit Changpinyo, Piyush Sharma, Nan Ding, and Radu Soricut. Conceptual 12m: Pushing web-scale image-text pre-training to recognize long-tail visual concepts. In *IEEE Conference on Computer Vision and Pattern Recognition, CVPR 2021, virtual, June 19-25, 2021*, pages 3558–3568. Computer Vision Foundation / IEEE, 2021.

[Chen *et al.*, 2019] Wei-Yu Chen, Yen-Cheng Liu, Zsolt Kira, Yu-Chiang Frank Wang, and Jia-Bin Huang. A closer look at few-shot classification. In *7th International Conference on Learning Representations, ICLR 2019, New Orleans, LA, USA, May 6-9, 2019*. OpenReview.net, 2019.

[Chen *et al.*, 2021a] Yinbo Chen, Zhuang Liu, Huijuan Xu, Trevor Darrell, and Xiaolong Wang. Meta-baseline: Exploring simple meta-learning for few-shot learning. In *2021 IEEE/CVF International Conference on Computer Vision, ICCV 2021, Montreal, QC, Canada, October 10-17, 2021*, pages 9042–9051. IEEE, 2021.

[Chen *et al.*, 2021b] Zhi Chen, Yadan Luo, Ruihong Qiu, Sen Wang, Zi Huang, Jingjing Li, and Zheng Zhang. Semantics disentangling for generalized zero-shot learning. In *2021 IEEE/CVF International Conference on Computer Vision, ICCV 2021, Montreal, QC, Canada, October 10-17, 2021*, pages 8692–8700. IEEE, 2021.

[Chen *et al.*, 2023a] Haoxing Chen, Huaxiong Li, Yaohui Li, and Chunlin Chen. Sparse spatial transformers for few-shot learning. *Sci. China Inf. Sci.*, 66(11), 2023.

[Chen *et al.*, 2023b] Wentao Chen, Chenyang Si, Zhang Zhang, Liang Wang, Zilei Wang, and Tieniu Tan. Semantic prompt for few-shot image recognition. *CoRR*, abs/2303.14123, 2023.

[Chen *et al.*, 2023c] Zhi Chen, Yadan Luo, Sen Wang, Jingjing Li, and Zi Huang. Gsmflow: Generation shifts mitigating flow for generalized zero-shot learning. *IEEE Trans. Multim.*, 25:5374–5385, 2023.

[Chen *et al.*, 2023d] Zhi Chen, Peng-Fei Zhang, Jingjing Li, Sen Wang, and Zi Huang. Zero-shot learning by harnessing adversarial samples. In Abdulmotaleb El-Saddik, Tao Mei, Rita Cucchiara, Marco Bertini, Diana Patricia Tobon Vallejo, Pradeep K. Atrey, and M. Shamim Hossain, editors, *Proceedings of the 31st ACM International Conference on Multimedia, MM 2023, Ottawa, ON, Canada, 29 October 2023- 3 November 2023*, pages 4138–4146. ACM, 2023.

[Chen *et al.*, 2024] Derong Chen, Feiyu Chen, Deqiang Ouyang, and Jie Shao. Mutual correlation network for few-shot learning. *Neural Networks*, 175:106289, 2024.

[Chen *et al.*, 2025a] Lingxing Chen, Yang Gu, Yi Guo, Fan Dong, Dongmei Jiang, and Yiqiang Chen. DDC: dynamic distribution calibration for few-shot learning under multi-scale representation. *Knowl. Based Syst.*, 311:113030, 2025.

[Chen *et al.*, 2025b] Xingye Chen, Wenxiao Wu, Li Ma, Xinge You, Changxin Gao, Nong Sang, and Yuanjie Shao. Exploring sample relationship for few-shot classification. *Pattern Recognit.*, 159:111089, 2025.

[Chen *et al.*, 2025c] Zhi Chen, Zecheng Zhao, Jingcai Guo, Jingjing Li, and Huang Zi. Svip: Semantically contextualized visual patches for zero-shot learning. In *Proceedings of the IEEE/CVF international conference on computer vision*, pages 3346–3356, 2025.

[Chen *et al.*, 2026] Zhi Chen, Xin Yu, Xiaohui Tao, Yan Li, and Zi Huang. Cluster-aware prompt ensemble learning for few-shot vision-language model adaptation. *Pattern Recognit.*, 172:112596, 2026.

[Cheng *et al.*, 2023] Hao Cheng, Siyuan Yang, Joey Tianyi Zhou, Lanqing Guo, and Bihan Wen. Frequency guidance matters in few-shot learning. In *IEEE/CVF International Conference on Computer Vision, ICCV 2023, Paris, France, October 1-6, 2023*, pages 11780–11790. IEEE, 2023.

[Cumplido *et al.*, 2025] Javier Ródenas Cumplido, Eduardo Aguilera, and Petia Radeva. Slot attention-based feature filtering for few-shot learning. In *IEEE/CVF Conference on Computer Vision and Pattern Recognition Workshops, CVPR Workshops 2025, Nashville, TN, USA, June 11-15, 2025*, pages 30–40. Computer Vision Foundation / IEEE, 2025.

[Dong *et al.*, 2025] Mengping Dong, Fei Li, Zhenbo Li, and Xue Liu. PRSN: prototype resynthesis network with cross-image semantic alignment for few-shot image classification. *Pattern Recognit.*, 159:111122, 2025.

[Finn *et al.*, 2017] Chelsea Finn, Pieter Abbeel, and Sergey Levine. Model-agnostic meta-learning for fast adaptation of deep networks. In Doina Precup and Yee Whye Teh, editors, *Proceedings of the 34th International Conference on Machine Learning, ICML 2017, Sydney, NSW, Australia, 6-11 August 2017*, volume 70 of *Proceedings of Machine Learning Research*, pages 1126–1135. PMLR, 2017.

[Fu *et al.*, 2023] Yuqian Fu, Yu Xie, Yanwei Fu, and Yu-Gang Jiang. Styleadv: Meta style adversarial training for cross-domain few-shot learning. In *IEEE/CVF Conference on Computer Vision and Pattern Recognition, CVPR 2023, Vancouver, BC, Canada, June 17-24, 2023*, pages 24575–24584. IEEE, 2023.

[Fu *et al.*, 2025] Meijun Fu, Xiaomin Wang, Jun Wang, and Zhang Yi. Prototype bayesian meta-learning for few-shot image classification. *IEEE Trans. Neural Networks Learn. Syst.*, 36(4):7010–7024, 2025.

[Guo and Guo, 2020] Jingcai Guo and Song Guo. A novel perspective to zero-shot learning: Towards an alignment of manifold structures via semantic feature expansion. *IEEE Transactions on Multimedia*, 23:524–537, 2020.

[Guo *et al.*, 2021] Jingcai Guo, Song Guo, Shiheng Ma, Yuxia Sun, and Yuanyuan Xu. Conservative novelty synthesizing network for malware recognition in an open-set scenario. *IEEE Transactions on Neural Networks and Learning Systems*, 34(2):662–676, 2021.

[Guo *et al.*, 2023] Jingcai Guo, Song Guo, Qihua Zhou, Ziming Liu, Xiaocheng Lu, and Fushuo Huo. Graph knows unknowns: Reformulate zero-shot learning as sample-level graph recognition. In *Proceedings of the AAAI conference on artificial intelligence*, pages 7775–7783. AAAI Press, 2023.

[Guo *et al.*, 2024a] Jingcai Guo, Zhijie Rao, Zhi Chen, Jingen Zhou, and Dacheng Tao. Fine-grained zero-shot learning: Advances, challenges, and prospects. *arXiv preprint arXiv:2401.17766*, 2024.

[Guo *et al.*, 2024b] Jingcai Guo, Han Wang, Yuanyuan Xu, Wenchao Xu, Yufeng Zhan, Yuxia Sun, and Song Guo. Multimodal dual-embedding networks for malware open-set recognition. *IEEE Transactions on Neural Networks and Learning Systems*, 36(3):4545–4559, 2024.

[Guo *et al.*, 2024c] Jingcai Guo, Qihua Zhou, Xiaocheng Lu, Ruibin Li, Ziming Liu, Jie Zhang, Bo Han, Junyang Chen, Xin Xie, and Song Guo. Parsnets: A parsimonious composition of orthogonal and low-rank linear networks for zero-shot learning. In *Proceedings of the Thirty-Third International Joint Conference on Artificial Intelligence, IJCAI-24*, pages 4062–4070, 2024.

[Hao *et al.*, 2023] Fusheng Hao, Fengxiang He, Liu Liu, Fuxiang Wu, Dacheng Tao, and Jun Cheng. Class-aware patch embedding adaptation for few-shot image classification. In *IEEE/CVF International Conference on Computer Vision, ICCV 2023, Paris, France, October 1-6, 2023*, pages 18859–18869. IEEE, 2023.

[He *et al.*, 2016] Kaiming He, Xiangyu Zhang, Shaoqing Ren, and Jian Sun. Deep residual learning for image recognition. In *Proceedings of the IEEE conference on computer vision and pattern recognition*, pages 770–778, 2016.

[He *et al.*, 2023] Ju He, Adam Kortylewski, and Alan Yuille. Corl: Compositional representation learning for few-shot classification. In *Proceedings of the IEEE/CVF Winter Conference on Applications of Computer Vision (WACV)*, pages 3890–3899, January 2023.

[Hu and Ma, 2022] Yanxu Hu and Andy J. Ma. Adversarial feature augmentation for cross-domain few-shot classification. In Shai Avidan, Gabriel J. Brostow, Moustapha Cissé, Giovanni Maria Farinella, and Tal Hassner, editors, *Computer Vision - ECCV 2022 - 17th European Conference, Tel Aviv, Israel, October 23-27, 2022, Proceedings, Part XX*, volume 13680 of *Lecture Notes in Computer Science*, pages 20–37. Springer, 2022.

[Krishna *et al.*, 2017] Ranjay Krishna, Yuke Zhu, Oliver Groth, Justin Johnson, Kenji Hata, Joshua Kravitz, Stephanie Chen, Yannis Kalantidis, Li-Jia Li, David A. Shamma, Michael S. Bernstein, and Li Fei-Fei. Visual genome: Connecting language and vision using crowd-sourced dense image annotations. *Int. J. Comput. Vis.*, 123(1):32–73, 2017.

[Lee *et al.*, 2019] Kwonjoon Lee, Subhransu Maji, Avinash Ravichandran, and Stefano Soatto. Meta-learning with differentiable convex optimization. In *IEEE Conference on Computer Vision and Pattern Recognition, CVPR 2019, Long Beach, CA, USA, June 16-20, 2019*, pages 10657–10665. Computer Vision Foundation / IEEE, 2019.

[Li and Wang, 2023] Zhuoling Li and Yong Wang. Better integrating vision and semantics for improving few-shot classification. In Abdulmotaleb El-Saddik, Tao Mei, Rita Cucchiara, Marco Bertini, Diana Patricia Tobon Vallejo, Pradeep K. Atrey, and M. Shamim Hossain, editors, *Proceedings of the 31st ACM International Conference on Multimedia, MM 2023, Ottawa, ON, Canada, 29 October 2023- 3 November 2023*, pages 4737–4746. ACM, 2023.

[Li *et al.*, 2022] Junnan Li, Dongxu Li, Caiming Xiong, and Steven C. H. Hoi. BLIP: bootstrapping language-image pre-training for unified vision-language understanding and generation. In Kamalika Chaudhuri, Stefanie Jegelka, Le Song, Csaba Szepesvári, Gang Niu, and Sivan Sabato, editors, *International Conference on Machine Learning, ICML 2022, 17-23 July 2022, Baltimore, Maryland, USA*, volume 162 of *Proceedings of Machine Learning Research*, pages 12888–12900. PMLR, 2022.

[Li *et al.*, 2025] Wenhao Li, Qiangchang Wang, Xianjing Meng, Zhibin Wu, and Yilong Yin. VT-FSL: bridging vision and text with llms for few-shot learning. *CoRR*, abs/2509.25033, 2025.

[Lin *et al.*, 2014] Tsung-Yi Lin, Michael Maire, Serge J. Belongie, James Hays, Pietro Perona, Deva Ramanan, Piotr Dollár, and C. Lawrence Zitnick. Microsoft COCO: common objects in context. In David J. Fleet, Tomás Pajdla, Bernt Schiele, and Tinne Tuytelaars, editors, *Computer Vision - ECCV 2014 - 13th European Conference, Zurich, Switzerland, September 6-12, 2014, Proceedings, Part V*, pages 747–762. Springer, 2014.

volume 8693 of *Lecture Notes in Computer Science*, pages 740–755. Springer, 2014.

[Liu *et al.*, 2021] Ze Liu, Yutong Lin, Yue Cao, Han Hu, Yixuan Wei, Zheng Zhang, Stephen Lin, and Baining Guo. Swin transformer: Hierarchical vision transformer using shifted windows. In *2021 IEEE/CVF International Conference on Computer Vision, ICCV 2021, Montreal, QC, Canada, October 10-17, 2021*, pages 9992–10002. IEEE, 2021.

[Liu *et al.*, 2023] Xinyue Liu, Ligang Liu, Han Liu, and Xiaotong Zhang. Capturing the few-shot class distribution: Transductive distribution optimization. *Pattern Recognit.*, 138:109371, 2023.

[Lu *et al.*, 2023] Xiaocheng Lu, Song Guo, Ziming Liu, and Jingcai Guo. Decomposed soft prompt guided fusion enhancing for compositional zero-shot learning. In *Proceedings of the IEEE/CVF Conference on Computer Vision and Pattern Recognition*, pages 23560–23569, 2023.

[Luo *et al.*, 2023] Xu Luo, Hao Wu, Ji Zhang, Lianli Gao, Jing Xu, and Jingkuan Song. A closer look at few-shot classification again. In Andreas Krause, Emma Brunskill, Kyunghyun Cho, Barbara Engelhardt, Sivan Sabato, and Jonathan Scarlett, editors, *International Conference on Machine Learning, ICML 2023, 23-29 July 2023, Honolulu, Hawaii, USA*, volume 202 of *Proceedings of Machine Learning Research*, pages 23103–23123. PMLR, 2023.

[Ordonez *et al.*, 2011] Vicente Ordonez, Girish Kulkarni, and Tamara L. Berg. Im2text: Describing images using 1 million captioned photographs. In John Shawe-Taylor, Richard S. Zemel, Peter L. Bartlett, Fernando C. N. Pereira, and Kilian Q. Weinberger, editors, *Advances in Neural Information Processing Systems 24: 25th Annual Conference on Neural Information Processing Systems 2011. Proceedings of a meeting held 12-14 December 2011, Granada, Spain*, pages 1143–1151, 2011.

[Oreshkin *et al.*, 2018] Boris N. Oreshkin, Pau Rodríguez López, and Alexandre Lacoste. TADAM: task dependent adaptive metric for improved few-shot learning. In Samy Bengio, Hanna M. Wallach, Hugo Larochelle, Kristen Grauman, Nicolò Cesa-Bianchi, and Roman Garnett, editors, *Advances in Neural Information Processing Systems 31: Annual Conference on Neural Information Processing Systems 2018, NeurIPS 2018, December 3-8, 2018, Montréal, Canada*, pages 719–729, 2018.

[Peng *et al.*, 2019] Zhimao Peng, Zechao Li, Junge Zhang, Yan Li, Guo-Jun Qi, and Jinhui Tang. Few-shot image recognition with knowledge transfer. In *2019 IEEE/CVF International Conference on Computer Vision, ICCV 2019, Seoul, Korea (South), October 27 - November 2, 2019*, pages 441–449. IEEE, 2019.

[Radford *et al.*, 2021] Alec Radford, Jong Wook Kim, Chris Hallacy, Aditya Ramesh, Gabriel Goh, Sandhini Agarwal, Girish Sastry, Amanda Askell, Pamela Mishkin, Jack Clark, Gretchen Krueger, and Ilya Sutskever. Learning transferable visual models from natural language supervision. In Marina Meila and Tong Zhang, editors, *Proceedings of the 38th International Conference on Machine Learning, ICML 2021, 18-24 July 2021, Virtual Event*, volume 139 of *Proceedings of Machine Learning Research*, pages 8748–8763. PMLR, 2021.

[Ren *et al.*, 2018] Mengye Ren, Eleni Triantafillou, Sachin Ravi, Jake Snell, Kevin Swersky, Joshua B. Tenenbaum, Hugo Larochelle, and Richard S. Zemel. Meta-learning for semi-supervised few-shot classification. In *6th International Conference on Learning Representations, ICLR 2018, Vancouver, BC, Canada, April 30 - May 3, 2018, Conference Track Proceedings*. OpenReview.net, 2018.

[Russakovsky *et al.*, 2015] Olga Russakovsky, Jia Deng, Hao Su, Jonathan Krause, Sanjeev Satheesh, Sean Ma, Zhiheng Huang, Andrej Karpathy, Aditya Khosla, Michael S. Bernstein, Alexander C. Berg, and Li Fei-Fei. Imagenet large scale visual recognition challenge. *Int. J. Comput. Vis.*, 115(3):211–252, 2015.

[Schuhmann *et al.*, 2021] Christoph Schuhmann, Richard Vencu, Romain Beaumont, Robert Kaczmarczyk, Clayton Mullis, Aarush Katta, Theo Coombes, Jenia Jitsev, and Aran Komatsuzaki. LAION-400M: open dataset of clip-filtered 400 million image-text pairs. *CoRR*, abs/2111.02114, 2021.

[Snell *et al.*, 2017] Jake Snell, Kevin Swersky, and Richard S. Zemel. Prototypical networks for few-shot learning. In Isabelle Guyon, Ulrike von Luxburg, Samy Bengio, Hanna M. Wallach, Rob Fergus, S. V. N. Vishwanathan, and Roman Garnett, editors, *Advances in Neural Information Processing Systems 30: Annual Conference on Neural Information Processing Systems 2017, December 4-9, 2017, Long Beach, CA, USA*, pages 4077–4087, 2017.

[Sung *et al.*, 2018] Flood Sung, Yongxin Yang, Li Zhang, Tao Xiang, Philip H. S. Torr, and Timothy M. Hospedales. Learning to compare: Relation network for few-shot learning. In *2018 IEEE Conference on Computer Vision and Pattern Recognition, CVPR 2018, Salt Lake City, UT, USA, June 18-22, 2018*, pages 1199–1208. Computer Vision Foundation / IEEE Computer Society, 2018.

[Tang *et al.*, 2025] Hao Tang, Shengfeng He, and Jing Qin. Connecting giants: Synergistic knowledge transfer of large multimodal models for few-shot learning. In *Proceedings of the Thirty-Fourth International Joint Conference on Artificial Intelligence, IJCAI 2025, Montreal, Canada, August 16-22, 2025*, pages 6227–6235. ijcai.org, 2025.

[Tian *et al.*, 2020] Yonglong Tian, Yue Wang, Dilip Krishnan, Joshua B. Tenenbaum, and Phillip Isola. Rethinking few-shot image classification: A good embedding is all you need? In Andrea Vedaldi, Horst Bischof, Thomas Brox, and Jan-Michael Frahm, editors, *Computer Vision - ECCV 2020 - 16th European Conference, Glasgow, UK, August 23-28, 2020, Proceedings, Part XIV*, volume 12359 of *Lecture Notes in Computer Science*, pages 266–282. Springer, 2020.

[Tseng *et al.*, 2020] Hung-Yu Tseng, Hsin-Ying Lee, Jia-Bin Huang, and Ming-Hsuan Yang. Cross-domain few-shot classification via learned feature-wise transformation. In *8th International Conference on Learning Representations, ICLR 2020, Addis Ababa, Ethiopia, April 26-30, 2020*. OpenReview.net, 2020.

[Vinyals *et al.*, 2016] Oriol Vinyals, Charles Blundell, Tim Lillicrap, Koray Kavukcuoglu, and Daan Wierstra. Matching networks for one shot learning. In Daniel D. Lee, Masashi Sugiyama, Ulrike von Luxburg, Isabelle Guyon, and Roman Garnett, editors, *Advances in Neural Information Processing Systems 29: Annual Conference on Neural Information Processing Systems 2016, December 5-10, 2016, Barcelona, Spain*, pages 3630–3638, 2016.

[Wang *et al.*, 2019] Yan Wang, Wei-Lun Chao, Kilian Q. Weinberger, and Laurens van der Maaten. Simpleshot: Revisiting nearest-neighbor classification for few-shot learning. *CoRR*, abs/1911.04623, 2019.

[Wang *et al.*, 2023a] Runqi Wang, Hao Zheng, Xiaoyue Duan, Jianzhuang Liu, Yuning Lu, Tian Wang, Songcen Xu, and Baochang Zhang. Few-shot learning with visual distribution calibration and cross-modal distribution alignment. In *IEEE/CVF Conference on Computer Vision and Pattern Recognition, CVPR 2023, Vancouver, BC, Canada, June 17-24, 2023*, pages 23445–23454. IEEE, 2023.

[Wang *et al.*, 2023b] Xixi Wang, Xiao Wang, Bo Jiang, and Bin Luo. Few-shot learning meets transformer: Unified query-support transformers for few-shot classification. *IEEE Trans. Circuits Syst. Video Technol.*, 33(12):7789–7802, 2023.

[Wu and Hu, 2022] Jiaying Wu and Jinglu Hu. Improved prior selection using semantics in maximum a posteriori for few-shot learning. *Knowl. Based Syst.*, 237:107688, 2022.

[Wu *et al.*, 2021] Jiaying Wu, Ning Dong, Fan Liu, Sai Yang, and Jinglu Hu. Feature hallucination via maximum A posteriori for few-shot learning. *Knowl. Based Syst.*, 225:107129, 2021.

[Xing *et al.*, 2019] Chen Xing, Negar Rostamzadeh, Boris N. Oreshkin, and Pedro O. Pinheiro. Adaptive cross-modal few-shot learning. In Hanna M. Wallach, Hugo Larochelle, Alina Beygelzimer, Florence d’Alché-Buc, Emily B. Fox, and Roman Garnett, editors, *Advances in Neural Information Processing Systems 32: Annual Conference on Neural Information Processing Systems 2019, NeurIPS 2019, December 8-14, 2019, Vancouver, BC, Canada*, pages 4848–4858, 2019.

[Yang *et al.*, 2021] Shuo Yang, Lu Liu, and Min Xu. Free lunch for few-shot learning: Distribution calibration. In *9th International Conference on Learning Representations, ICLR 2021, Virtual Event, Austria, May 3-7, 2021*. OpenReview.net, 2021.

[Yang *et al.*, 2022a] Fengyuan Yang, Ruiping Wang, and Xilin Chen. SEGA: semantic guided attention on visual prototype for few-shot learning. In *IEEE/CVF Winter Conference on Applications of Computer Vision, WACV 2022, Waikoloa, HI, USA, January 3-8, 2022*, pages 1586–1596. IEEE, 2022.

[Yang *et al.*, 2022b] Shuo Yang, Songhua Wu, Tongliang Liu, and Min Xu. Bridging the gap between few-shot and many-shot learning via distribution calibration. *IEEE Trans. Pattern Anal. Mach. Intell.*, 44(12):9830–9843, 2022.

[Yang *et al.*, 2023] Fengyuan Yang, Ruiping Wang, and Xilin Chen. Semantic guided latent parts embedding for few-shot learning. In *IEEE/CVF Winter Conference on Applications of Computer Vision, WACV 2023, Waikoloa, HI, USA, January 2-7, 2023*, pages 5436–5446. IEEE, 2023.

[Yue *et al.*, 2025] Ling Yue, Lin Feng, Qiuping Shuai, Zihao Li, and Lingxiao Xu. Multi-level adaptive feature representation based on task augmentation for cross-domain few-shot learning. *Appl. Intell.*, 55(4):291, 2025.

[Zhang *et al.*, 2024a] Hai Zhang, Junzhe Xu, Shanlin Jiang, and Zhenan He. Simple semantic-aided few-shot learning. In *IEEE/CVF Conference on Computer Vision and Pattern Recognition, CVPR 2024, Seattle, WA, USA, June 16-22, 2024*, pages 28588–28597. IEEE, 2024.

[Zhang *et al.*, 2024b] Tiange Zhang, Qing Cai, Feng Gao, Lin Qi, and Junyu Dong. Exploring cross-domain few-shot classification via frequency-aware prompting. In *Proceedings of the Thirty-Third International Joint Conference on Artificial Intelligence, IJCAI 2024, Jeju, South Korea, August 3-9, 2024*, pages 5490–5498. ijcai.org, 2024.

[Zhang *et al.*, 2025] Yourun Zhang, Maoguo Gong, Jianzhao Li, Kaiyuan Feng, and Mingyang Zhang. Few-shot learning with enhancements to data augmentation and feature extraction. *IEEE Trans. Neural Networks Learn. Syst.*, 36(4):6655–6668, 2025.

[Zhao *et al.*, 2024] Peng Zhao, Yin Wang, Wei Wang, Jie Mu, Huiting Liu, Cong Wang, and Xiaochun Cao. Multi-attention based visual-semantic interaction for few-shot learning. In *Proceedings of the Thirty-Third International Joint Conference on Artificial Intelligence, IJCAI 2024, Jeju, South Korea, August 3-9, 2024*, pages 1753–1761. ijcai.org, 2024.

[Zhou *et al.*, 2023] Fei Zhou, Peng Wang, Lei Zhang, Wei Wei, and Yanning Zhang. Revisiting prototypical network for cross domain few-shot learning. In *IEEE/CVF Conference on Computer Vision and Pattern Recognition, CVPR 2023, Vancouver, BC, Canada, June 17-24, 2023*, pages 20061–20070. IEEE, 2023.

[Zhou *et al.*, 2025] Chunpeng Zhou, Zhi Yu, Xilu Yuan, Sheng Zhou, Jiajun Bu, and Haishuai Wang. Less is more: A closer look at semantic-based few-shot learning. *Inf. Fusion*, 114:102672, 2025.

[Zou *et al.*, 2024] Yixiong Zou, Yicong Liu, Yiman Hu, Yuhua Li, and Ruixuan Li. Flatten long-range loss landscapes for cross-domain few-shot learning. In *IEEE/CVF Conference on Computer Vision and Pattern Recognition, CVPR 2024, Seattle, WA, USA, June 16-22, 2024*, pages 23575–23584. IEEE, 2024.